

# DESIGN AND MODELING OF A PIEZOELECTRICALLY ACTUATED MICROVALVE

Micky RAKOTONDRABE<sup>1</sup>, Ioan Alexandru IVAN<sup>1,2</sup>, Valentin STIHI<sup>3</sup>, Simona NOVEANU<sup>4</sup>, Eugenia MINCA<sup>2</sup>

<sup>1</sup> FEMTO-ST Institute, AS2M Department, 24 Rue Alain Savary, Besancon, 25000, France, e-mails: [mrakoton@femto-st.fr](mailto:mrakoton@femto-st.fr), [alex.ivan@femto-st.fr](mailto:alex.ivan@femto-st.fr)

<sup>2</sup> Valahia Univ. of Targoviste, Electrical Eng. Faculty, Bd. Unirii 18-20, 130082, Targoviste, Romania, e-mails : [ivan@valahia.ro](mailto:ivan@valahia.ro), [minca@valahia.ro](mailto:minca@valahia.ro)

<sup>3</sup> Polytechnic Univ. of Bucharest, Electronics Telecommunications and IT Faculty, Bd. Iuliu Maniu 1-3, Bucharest, 061071, Romania, e-mail: [vstihi@yahoo.com](mailto:vstihi@yahoo.com)

<sup>4</sup> Technical Univ. of Cluj-Napoca, Department of Mechanisms, Precision Eng. and Mechatr., Bd. Muncii 103-105, Cluj-Napoca, 400641, Romania, e-mail: [simona.noveanu@mmfm.utcluj.ro](mailto:simona.noveanu@mmfm.utcluj.ro)

Abstract. In this paper, we propose and model a new microvalve design based on a unimorph piezoelectric bending cantilever. When the piezoelectric structure is electrically driven, the valve opens with precise angles allowing smooth flow control. In order to understand the whole system dynamic behavior, a physical model is developed. While the developed model is strongly nonlinear.

Key words: piezoelectric, actuator, microvalve, dynamic modeling.

## 1. INTRODUCTION

Electrovalves are usually actuated by solenoids. Their response time is often too big for fast switching applications and they offer discrete output only [1]. Using geared motors a continuous flow control is achieved but with the inconvenient of an even bigger idle time. Miniaturization of these valves is also technically challenging. Pneumatic valves [2] present similar challenges. Piezoelectrically driven valves began to develop as a viable alternative. Piezoceramic materials such as PZT (lead zirconate titanate) [3] provide high energy density and electromechanical coupling factor. Their bandwidth allows response time in millisecond order and extremely low power consumption under one milliwatt. Finally, the high resolution that piezoelectric materials provide is very compatible to the required accuracy in microvalves.

In this paper, we propose a new principle of microvalve based on piezoelectric PZT actuator. The objective is to obtain a very accurate and with a very high settling time. In order to understand the behavior of the whole system, we developed a model. While the developed model is strongly nonlinear, it has been simulated for different input conditioning.

The paper is organized as follows. In Section-2, we present the piezoelectrically actuated microvalve. Section-3 is dedicated to the modeling of the whole system.

## 2. PRINCIPLE OF THE PIEZOELECTRICALLY ACTUATED MICROVALVE

Let us consider a tube whose fluid outlets to an end-use vat. The objective is to control the flow  $q_o [m^3 / s]$  that comes into the vat. The natural way to adjust it is to vary the opening at the extremity of the tube. To perform that, we propose to use an end-effector (steel) actuated by a piezoelectric cantilever (piezocantilever) (Figure.1-a). Initially, while the piezocantilever is not electrically excited, the end-effector obstructs the tube and no flow goes out from it, i.e.  $q_o = 0$ . When a voltage is applied to the piezocantilever, it bends and the end-effector effectuates an angle  $\alpha [rad]$  allowing the output flow as in Figure.1-b. Figure.2 pictures the design of the piezoelectrically actuated microvalve.

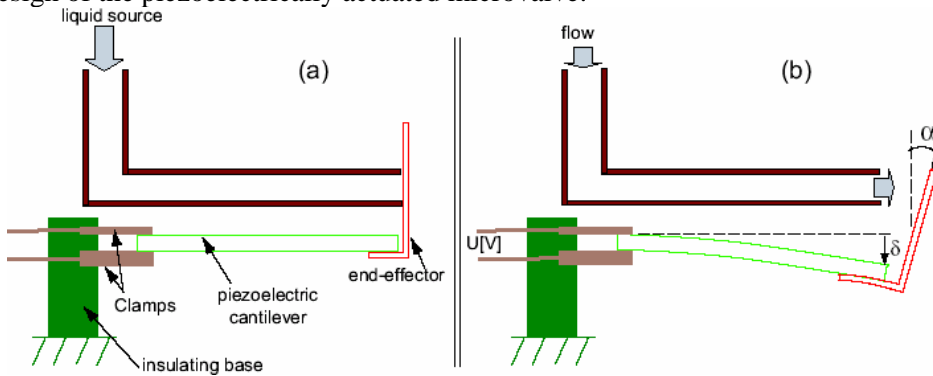


Figure 1 - Principle of the system.

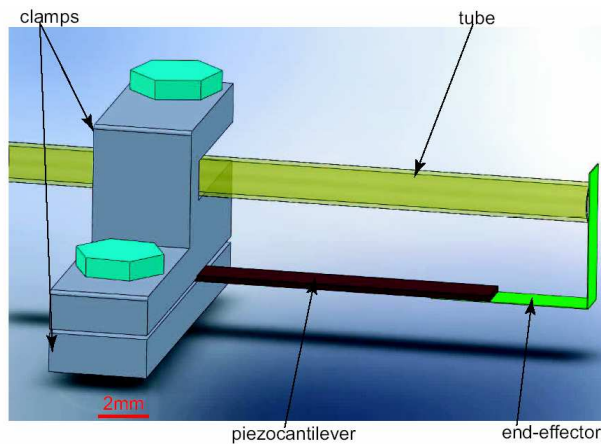


Figure 2 - Design of the piezoelectrically-actuated microvalve.

### 3. MODELING OF THE SYSTEM

This section is dedicated to provide the behavior equations of the system. The considered input control is the voltage applied to the piezocantilever, while the output is the flow  $q_o$ . The modeling is separated into three parts. First we model the piezocantilever. Afterwards, we give the equation that the end-effector plays. Then, we give the equation of the fluid flow part. Finally, we give the governing equations of the whole system.

#### 3.1 Equation of the piezocantilever

A piezocantilever is made up of one or more piezoelectric layers and one or more passive layers. Unimorph piezocantilevers, which are composed of one piezolayer and one passive layer, are appreciated because of their ease of mass production. In this study, we particularly use a PZT-layer and Copper-layer. When an external voltage is applied to the PZT-layer, it expands (or contracts) that leads to a bending  $\delta$  [ $\mu\text{m}$ ] of the piezocantilever (Figure.3).

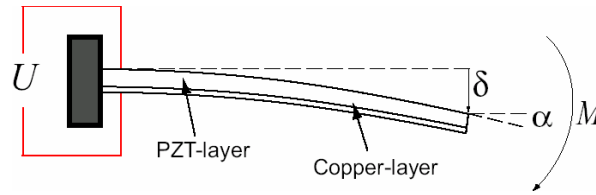


Figure 3 - A unimorph piezocantilever subjected to a voltage excitation.

Smits and Choi [4] provided static equations for the unimorph piezocantilever tip deflection  $\delta$  and the angle  $\alpha$  for a given voltage  $U$  and a mechanical momentum  $M$  :

$$\begin{cases} \alpha = m_{11}M + m_{12}U \\ \delta = m_{21}M + m_{22}U \end{cases} \quad (1)$$

where

$$m_{11} = \frac{12AL}{KW}, \quad m_{12} = -\frac{6Ad_{31}BL}{K}, \quad m_{21} = \frac{6AL^2}{KW}, \quad m_{22} = -\frac{3Ad_{31}BL^2}{K}$$

and

$$A = s_{11}^c s_{11}^p (s_{11}^c h_p + s_{11}^p h_c), \quad B = \frac{h_c (h_p + h_c)}{(s_{11}^c h_p + s_{11}^p h_c)}$$

$$K = (s_{11}^c)^2 (h_p)^4 + 4s_{11}^c s_{11}^p h_c (h_p)^3 + 6s_{11}^c s_{11}^p (h_c)^2 (h_p)^2 + 4s_{11}^c s_{11}^p h_p (h_c)^3 + (s_{11}^p)^2 (h_c)^4$$

$L$  and  $w$  are the respective length and width of piezocantilever while  $h_c$  and  $h_p$  are the thickness of the copper and PZT layers respectively. Their compliance coefficients are  $s_{11}^c$  and  $s_{11}^p$  respectively. Finally,  $d_{31}$  gives the transverse piezoelectric coefficient of the PZT material.

Equations (1) represent the static model of the piezocantilever. It has been shown that a second-order model is well adapted to approximate the dynamic part of such an actuator [5]. Introducing the dynamic part, we finally have:

$$\begin{cases} a_\alpha \frac{d^2 \alpha}{dt^2} + b_\alpha \frac{d\alpha}{dt} + \alpha = m_{11}M + m_{12}U \\ a_\delta \frac{d^2 \delta}{dt^2} + b_\delta \frac{d\delta}{dt} + \delta = m_{21}M + m_{22}U \end{cases} \quad (2)$$

where  $a_i$  and  $b_i$  ( $i \in \{\alpha, \delta\}$ ) are the inertial and damping coefficients respectively.

While  $\delta$  and  $\alpha$  can be considered as internal states of the actuator, the momentum  $M$  is unknown. The next subsection is focused on the expression of  $M$  by using the geometrical modeling of the end-effector.

### 3.2 Equation of the momentum by modeling the end-effector

Figure.4 pictures a simplified scheme of the piezocantilever and related end-effector. Initially, the outlet of the tube is at the distance  $L_{ao}$  of the tube axis. When the piezocantilever bends,  $L_a$  denotes the new distance. The amplitude of the force applied by the fluid to the end-effector is  $F$ .

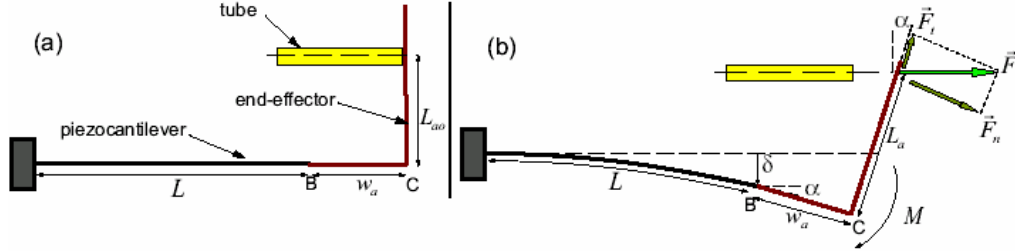


Figure 4 - Simplified scheme of the system.

The expression of the momentum is:

$$M \approx F_n L_a - F_t (L + w_a) \quad (3)$$

where the tangential and normal components of the force are:  $F_t = F \sin(\alpha)$  and  $F_n = F \cos(\alpha)$  respectively.

On the other hand, based on the figure.4-b, the distance  $L_a$  can be expressed as follows:

$$L_a = \frac{1}{\cos(\alpha)} (L_{ao} + \delta + w_a \sin(\alpha)) \quad (4)$$

Inserting Equa.(4) and the components of the force into Equa.(3), we derive the expression of the momentum:

$$M \approx (L_{ao} + \delta - L \sin(\alpha)) F \quad (5)$$

The force  $F$  is unknown, it can be expressed by calculating the one applied by the fluid on the end-effector which is called jet force. This is the aim of the next subsection.

### 3.3 Equation of the force by modeling the jet force

Consider the figure.5 where the interaction between the end-effector and the fluid from the tube is zoomed. The diameter of the tube is  $d_a$ . At its extremity, the flow, the pressure and the speed of the fluid are denoted by  $q_A$ ,  $p_A$  and  $v_A$  respectively. They are supposed as known. When the end-effector turns, the tangential speed at distance  $L_a$  is  $v_{La} = L_a \frac{d\alpha}{dt}$ . The medium distance between the tube and the end-effector is denoted by  $d_s$ .

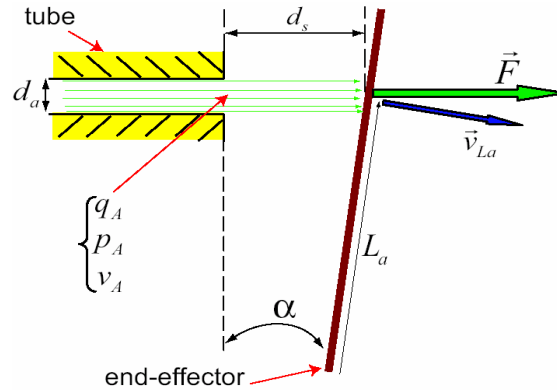


Figure 5 - Zoom of interaction between the end-effector and the fluid motion from the tube.

Using dynamic fluid motion law (see for example [6]), we have:

$$q_A (v_{La} \cos(\alpha) - v_A) = p_A S_A - F \quad (6)$$

where  $S_A = \frac{\pi d_A^2}{4}$  is the section of the tube at its extremity. Replacing  $v_{La}$  by its expression and  $L_a$  by Equa.(4), we deduce the force:

$$F = p_A S_A - q_A \left( (L_{ao} + \delta + w_a \sin(\alpha)) \frac{d\alpha}{dt} - v_A \right) \quad (7)$$

### 3.4 Expression of the effective output flow $q_o$

The effective output flow  $q_o$  is considered as the fluid that comes out from the tube. It depends on the opening gap  $d_s$  between the tube and the end-effector. We have:

$$q_o = S_o v_A \quad (8)$$

where  $S_o \approx \pi d_A d_s$  is the side area of the fluid between the tube and the end-effector. Using  $d_s = L_a \sin(\alpha)$  and replacing  $L_a$ , we finally have:

$$q_o = \pi d_A \tan(\alpha) (L_{ao} + \delta + w_a \sin(\alpha)) \quad (9)$$

## 4. SIMULATION

### 4.1 The final model

Based on the previous section, the final model that governs the piezoelectrically actuated microvalve is given by the following strongly nonlinear dynamic model to be introduced into Simulink:

$$\left\{ \begin{array}{l} a_\alpha \frac{d^2 \alpha}{dt^2} + b_\alpha \frac{d\alpha}{dt} + \alpha = m_{11} M + m_{12} U \\ a_\delta \frac{d^2 \delta}{dt^2} + b_\delta \frac{d\delta}{dt} + \delta = m_{21} M + m_{22} U \\ M = (L_{ao} + \delta - L \sin(\alpha)) F \\ F = p_A S_A - q_A \left( (L_{ao} + \delta + w_a \sin(\alpha)) \frac{d\alpha}{dt} - v_A \right) \\ q_o = \pi d_A \tan(\alpha) (L_{ao} + \delta + w_a \sin(\alpha)) \end{array} \right. \quad (10)$$

Matlab/Simulink simulation parameters (fluid is water):

```

s11c=1/110e9;    %1/Pa          bdelta=1.304e-5;    %s
s11p=16.5e-12;  %1/Pa          Lao=5e-3;          %m
d31=-260e-12;   %N/C          wa=3e-3;            %m
L=15e-3;        %m             dA=2e-3;            %m
w=2e-3;         %m             qA=2e-9;            %m3/s
hp=0.2e-3;      %m             pA=1600;            %Pa
hc=0.1e-3;      %m             Cdelta=[0 1 0 0];
adelta=4.722e-8;%s^2

```

## 4.2 Systemic scheme

Figure.6 pictures the systemic scheme of Equa.(8). It describes how the different coupling and effects are connected. In the figure, the term  $\frac{d\alpha}{dt}$  can be derived either from the derivative of  $\alpha$  or by multiplication the state vector  $X$  with a matrix  $C_{d\alpha}$  such as:

$$X = \begin{pmatrix} \alpha \\ \frac{d\alpha}{dt} \\ \delta \\ \frac{d\delta}{dt} \end{pmatrix}, \quad C_{d\alpha} = \begin{pmatrix} 0 & 1 & 0 & 0 \end{pmatrix} \quad (11)$$

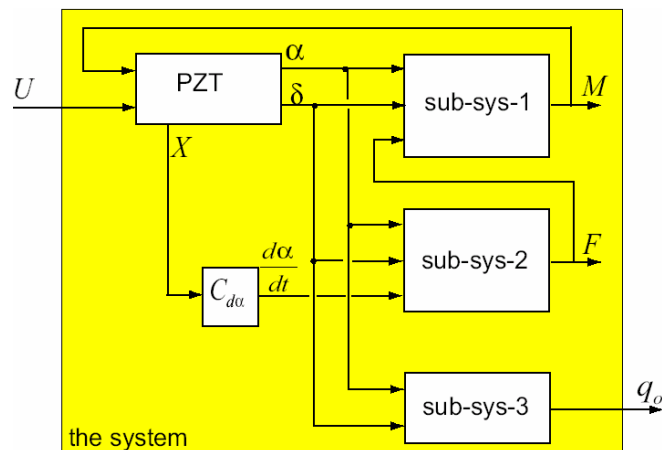


Figure 6 - State-space systemic scheme.

The state matrix  $X$  is available either by sensors or by using a state observer [7].

## 4.2 Simulation results

Actuator geometry insures that displacement and flow values are negative for positive applied voltages. At null voltage but for a given non-zero fluid pressure the model correctly provide a flow offset value. This can be avoided by a reverse voltage or by pre-compressing the end-effector. A control system would better work in closed-loop, incorporating at least one external sensor for hydrostatic pressure or directly for flow rate.

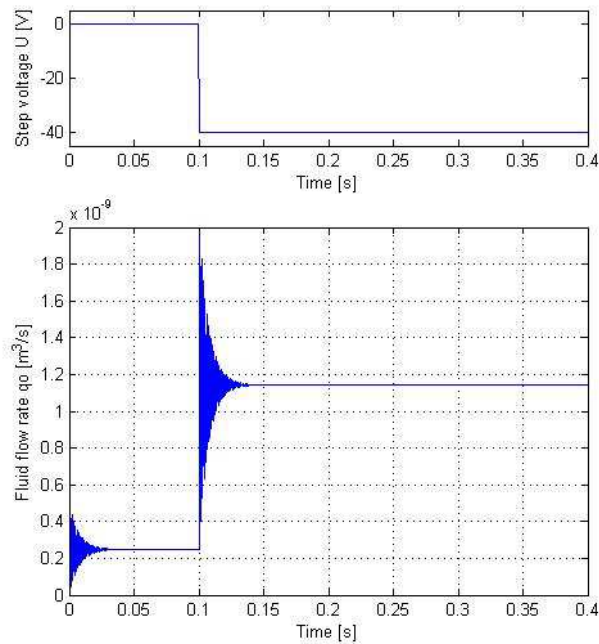
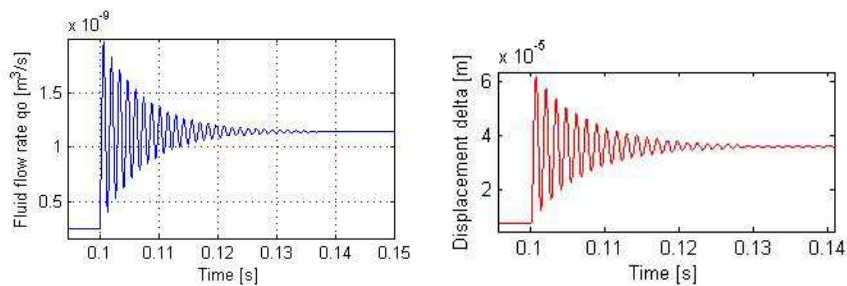


Figure 7 – Flow rate of a step response of an input signal of  $-40\text{V}$ .



Figures 8,9 – Zoom on flow rate and end-effector mechanical displacement.

Based on above geometry and input parameters, second-order simulation model provided that settling time is 20 ms. Static flow rate is  $-0.0228 \text{ mm}^3/\text{V}$  at

1600 Pa and related mechanical opening is 0.7mm/V. At null input voltage there is a constant flow of 15.6mm<sup>3</sup>/bar; a reverse voltage of 2.994 mV/Pa is required to compensate the hydrostatic pressure.

## 5. CONCLUSION

We proposed a fast piezoelectrically driven valve for controlling small fluid flows in a range of up to several cubic millimeter per second. Expected resolution may reach several dozens picoliters per second, depending on outlet diameter.

However we must admit that we used several simplifying hypothesis that should be further refined in the model, such as: ideal fluid (laminar flow, incompressible, no capillarity etc.), infinite end-effector stiffness, and linear piezoelectric material. Mechanical structure may be optimized with an appropriate damping to avoid actual significant flow overshoot and further improve response time.

## REFERENCES

- [1] Brian Nesbitt et. al., *Guide to European valves: for control, isolation and safety*, John Wiley and Sons, 2001
- [2] Peter Beater, *Pneumatic Drives: System Design, Modelling and Control*, Springer, 2007
- [3] A.J. Moulson and J.M. Herbert, *Electroceramics: Materials, Properties, Applications 2<sup>nd</sup> Edition*, John Wiley and Sons, 2003
- [4] J. G. Smits and W.S. Choi, *The constituent equations of piezoelectric heterogeneous bimorph*, IEEE Ultrasonic Symposium, 1990.
- [5] M. Rakotondrabe, C. Clévy and P. Lutz, *Complete open-loop control of hysteretic, creeped and oscillating piezoelectric cantileve*, IEEE Transactions on Automation Science and Engineering, accepted.
- [6] Franz Durst, *Fluid Mechanics, an introduction to the theory of fluid flows*, Springer, ISBN 978-3-540-71342-5, 2008.
- [7] D. G. Luenberger, *Observing the state of a linear system*, IEEE Transactions on Military Electronics, 1964.